EARTH SCIENCES
RESEARCH JOURNAL
Earth Sci. Res. J. Vol. 28, No. 3 (September, 2024): 349 - 359

UNIVERSIDAD NACIONAL DE COLOMBIA

HYDROGEOLOGY

Geo-electric techniques for estimating and mapping the electro-geohydraulic properties of the shallow aquifer within the Nsukka Formation in eastern Nigeria

Johnson C. Ibuot[1], Daniel N. Obiora[1], Moses M. M. Ekpa[2], and Emmanuel T. Omeje[1]
1. Department of Physics and Astronomy, University of Nigeria, Nsukka, Enugu State.
2. Federal College of Education (Technical), Omoku, Rivers State
*Corresponding author email: johnson.ibuot@unn.edu.ng

ABSTRACT

This study, employing Vertical Electrical Sounding (VES), was carried out within parts of Nsukka Formation located in southeastern Nigeria in order to determine the subsurface properties that aid in characterizing the subsurface. The study covers parts of Nsukka, Enugu Ezike, Obukpa and Eha Alumona in Enugu State, characterized by undulating terrain and a tropical climate with distinct wet and dry seasons. Twenty-one sounding data were acquired, and the measured data were quantitatively and qualitatively interpreted to determine the geoelectrical parameters. The interpreted resistivity curves revealed five geoelectric layers with different generic curve types. The secondary parameters estimated from modeled equations and their spatial distributions are displayed in the contour maps generated with Origin software. The estimated parameters - longitudinal conductance, transverse resistance, transverse resistivity, longitudinal resistivity, anisotropy, porosity, hydraulic conductivity, permeability, formation factor, and tortuosity-vary across the study area within the following ranges: 0.01 - 0.54, 373.90 - 11375.00, 109.56 - 5402.14, 108.72 - 4046.87, 1.01 - 1.88, 0.276 – 0.314, 0.187 – 3.509 m/day, 1.02E-5 - 9.32E-6 mD, 3.092 – 3.780, and 0.200 – 1.021, respectively. The variation of these parameters may be influenced by the heterogeneous nature of the subsurface. The regression analysis reveals the mutual relationships and correlation between the different parameters when plotted against each other. The results from this study are very promising, and demonstrate the efficacy of the geophysical approach in characterizing the subsurface for sustainable groundwater management and protection. The deployment of geo-electric indices in this study is to ensure adequate characterization of the subsurface.

Keywords: anisotropy; groundwater; geoelectric layer; resistivity; VES

Técnicas geoeléctricas para la estimación y mapeo de las propiedades electro-geohidráulicas en los acuíferos poco profundos en la formación Nsukka, en el este de Nigeria

RESUMEN

Este estudio, realizado con pruebas de Sondeo Eléctrico Vertical (SEV), se llevó a cabo en algunas partes de la Formación Nsukka, ubicada en el sudeste de Nigeria, para determinar las propiedades que ayuden a caracterizar el subsuelo de la formación. El estudio cubre partes de Nsukka, Enugu Ezike, Obukpa y Eha Alumona, en el estado de Enugu, caracterizado por terrenos ondulados y un clima tropical con distintas estaciones húmedas y secas. Se recolectó información de 21 sondeos y esta información se interpretó cuantitativa y cualitativamente para determinar los parámetros geoeléctricos. Las curvas interpretadas de resistividad revelaron cinco capas geoeléctricas con diferentes tipos de curvas genéricas. Los parámetros secundarios estimados a partir de las ecuaciones modeladas y sus distribuciones espaciales se presentan en los mapas de contornos generados con el software Origin. Los parámetros estimados -conductancia longitudinal, resistencia transversal, resistividad transversal, resistividad longitudinal, anisotropia, porosidad, conductividad hidráulica, permeabilidad, factor de formación y tortuosidad- varían a lo largo del área estudio dentro de los siguientes rangos 0.01 - 0.54, 373.90 - 11375.00, 109.56 - 5402.14, 108.72 - 4046.87, 1.01 - 1.88, 0.276 – 0.314, 0.187 – 3.509 m/day, 1.02E-5 - 9.32E-6 mD, 3.092 – 3.780, and 0.200 – 1.021, respectivamente. La variación de estos parámetros puede estar influenciada por la naturaleza heterogénea del subsuelo. El análisis de regresión revela una relación mutua y una correlación entre diferentes parámetros cuando se grafican entre sí. Los resultados de este estudio demuestran la eficacia de la aproximación geofísica en la caracterización del subsuelo para el manejo y la protección sostenible de las aguas subterráneas. El despliegue de índices geoeléctricos en este studio asegura una caracterización adecuada del subsuelo.

Palabras Claves: anisotropia; aguas subterráneas; capas geoeléctricas; Sondeo Eléctrico Vertical

Record
Manuscript received: 26/07/2023
Accepted for publication: 23/08/2024

How to cite item:
Ibuot, J. C., Obiora, D. N., Ekpa, M. M. M., & Omeje, E. T. (2024). Geo-electric techniques for estimating and mapping the electro-geohydraulic properties of the shallow aquifer within the Nsukka Formation in eastern Nigeria. *Earth Sciences Research Journal,* 28(3), 349-259. https://doi.org/10.15446/esrj.v28n3.110328

ISSN 1794-6190 e-ISSN 2339-3459
https://doi.org/10.15446/esrj.v28n3.110328

Introduction

The Earth's subsurface is made up of different naturally occurring materials, including minerals, rocks and soils. Extensive research underscores the indispensable role of water in supporting life, particularly plants and other organisms inhabiting soil ecosystems (Akpan et al., 2013; Ibanga and George. 2016; Obiora et al., 2016; Ibuot et al., 2019; George, 2020). Groundwater, as a fundamental natural resource, serves as the cornerstone for sustaining various human activities encompassing domestic, agricultural, industrial and social needs (Kelbe et al., 2011; Bricker et al., 2017). It is a vital component in preserving not only human existence but also the the diverse ecosystems reliant on it. The occurrence of groundwater is primarily dependent on geological, geomorphological and weathering factors, alongside rainfall patterns. The development of secondary porosity and permeability resulting from weathering and fracturing of parent rocks stands as a pivotal geological mechanism shaping aquifer repositories (Oli et al., 2020; Omeje et al., 2022a). The interaction of these factors leads to complex hydrogeological formations, characterized by variations in groundwater resources' quantity, quality, accessibility and renewability. Generally, groundwater exhibits high quality, owing to its substantial protection from surface contaminants facilitated by the natural purification processes occurring within the vadose zone (Ibuot et al., 2022; Nugraha et al 2021). A good knowledge of the aquifer systems is imperative to mitigate over-exploitation, which leads to borehole failures and groundwater pollution, thereby fostering environmental sustainability. Furthermore, the groundwater resources hold significant potential for enhancing livelihoods, notwithstanding the challenges and knowledge gaps concerning groundwater dynamics occurrence, flow and transmissibility.

The groundwater repository is controlled by the geometry of aquifers and interlayered aquitards, aquifer types (confined or unconfined), water table fluctuations, recharge and discharge sources, hydraulic properties derived from aquifer materials' characteristics. In the characterization of subsurface lithologic units, hydraulic properties such as permeability, porosity, tortuosity, transmissibility, tortuosity, hydraulic capillary radius, and surface area per unit volume serve as invaluable and dynamic tools that provide adequate information about the subsurface litho-textural characteristics (Ibuot et al., 2019; Ekanem et al., 2022; Omeje et al., 2022b; Asfahani and Al-Fares, 2021). Voids, pore spaces and fractures play pivotal roles in groundwater studies, influencing the flow dynamics within subsurface formations. Groundwater flow is significantly influenced by fractures, with multitude of evenly distributed fractures facilitating flow throughout the saturated layer. The flow of groundwater through fractures and fissures is characterized by heterogenic permeability and the heterogeneity affects the transmissibility properties of the aquifer (Niwas and Celik 2012; Asfahani and Al-Fares, 2022).

The geohydraulic properties of the aquifer units depend upon factors such as geometry, voids, grain sizes, and interconnection of the pores, facilitating the flow of accumulated water (George et al. 2015). Porosity, primarily influenced by grain arrangement, can reduce proportionally with increase in grain size; however, grain size itself does not affect total porosity in sediments of uniform (Mazac et al., 1985; Ekanem et al., 2022). The geohydraulic properties under scrutiny in this study, encompassing hydraulic conductivity, porosity, permeability, hydraulic capillary radius, surface area per unit volume, play pivotal roles in governing the water-bearing characteristics of hydrogeologic units. The spatial distribution and interplay of these properties aid in classifying aquifer units based on their transmissiblility and potentiality (George et al., 2015; Omeje et al., 2022a; Ibuot et al., 2024). Incorporating these properties is essential for characterizing aquifer units effectively. Parameters derived from resistivity data interpretation are corroborated with existing subsurface data to facilitate comparison and validation (George et al., 2015; Opara et al., 2020).

The scarcity of pumping test data owing to the high cost of measuring instruments and poor data management in developing countries, has led to the use of non-invasive and cost-effective geophysical methods for aquifer units characterization. Among this methods, direct current electrical resistivity techniques have gained prominence for estimating aquifer hydraulic properties (Obiora et al., 2015: Ibanga et al., 2016; Omeje et al., 2021). Electrical resistivity techniques are widely utilized in groundwater investigations to facilitate the exploration of groundwater resources. Fundamentally, electrical resistivity involves injecting current into the earth through electrodes, and subsequently monitoring and recording the earth's response to current propagation (Telford et al., 1990, Lowrie, 1997; Todd and Mays 2005). The Vertical electrical sounding (VES) technique employing, employing the Schlumberger electrode configuration, is particularly instrumental in characterizing subsurface formations efficiency (Asfahani and Al-Fares, 2022; Obiora and Ibuot, 2023). The interpretation of VES data is influenced by various environmental and geological factors, including mineral content, inter-granular compaction, porosity, and degree of water saturation in the rocks (Gonzalez-Alvarez et al., 2016 and Shishaye et al. 2019). Numerous studies have successfully determined aquifer hydraulic properties using surficial electrical resistivity techniques in different parts of the world (Niwas and Celik 2012; Metwaly et al. 2014; George et al., 2015;Umar and Igwe, 2019; Obiora and Ibuot, 2020; Oli et al. 2020; Ekwe et al. 2020; Ibuot et al., 2022). Hence, the application of geo-electric techniques will aid in estimating and mapping the electro-geohydraulic properties of aquifers in parts of Nsukka Formation, particularly considering the local variations in aquifer characteristics, subsurface lithology, and the influence of environmental and geological factors on resistivity measurements. This will lead to improved groundwater management and resource sustainability. The aim of this study is to utilize geo-electric techniques to estimate and map the electro-geohydraulic properties of the shallow aquifer within the Nsukka Formation in eastern Nigeria, and to explore the interrelationships among these properties.

Background theory and electro-geohydraulic parameters

The electro-geohydraulic parameters considered in this study are longitudinal conductance, transverse resistance, longitudinal resistivity, transverse resistivity, anisotropy, porosity, hydraulic conductivity, permeability, formation factor, tortuosity, hydraulic capillary and surface area per unit volume. These properties were estimated from the primary geo-electric data obtained from VES measurements. The primary geo-electric properties (resistivity, thickness and depth) were obtained using the vertical electrical sounding using Schlumberger electrode array. The electrical resistivity technique assumed the earth to be an isotropic homogeneous medium, and the measurement demonstrates the true magnitude of resistivity, which does not depend on the potential electrode distance used (Nugraha et al., 2021). The flow of current in conducting medium is governed by Ohm's law (Equation 1);

$$j = -\sigma \frac{dV}{dr} \quad (1)$$

Where j, σ, V and r are the current density, electrical conductivity, electrical potential, and distance

The flow of groundwater in a porous medium is governed by the Darcy's law, which is expressed in Equation 2;

$$q = -K \frac{dh}{dr} \quad (2)$$

Where q, K, and h are specific discharge, hydraulic conductivity and hydraulic head. These two equations (1 and 2) are similar in form and can be combined to give Equation 3 which reduces to Equation 4.

$$\frac{Kdh}{q} = \frac{\sigma dv}{jdh} \quad (3)$$

$$K = \left(\frac{q}{dh}\right)\left(\frac{dV}{j}\right)\sigma \quad (4)$$

According to Asfahani and Al-Fares (2022), the mechanisms that control the flow of electric current and groundwater are principally related to the similar lithological and physical conditions of the earth's subsurface.

- **Longitudinal conductance, transverse resistance, longitudinal resistivity, transverse resistivity and anisotropy**

The primary parameters that describe a geoelectric layer are the resistivity (ρ) and thickness (h), while the secondary geoelectric parameters are derived from the combination of these primary parameters. The secondary parameters are significant in describing the subsurface lithological and structural

characteristics with less doubt. The longitudinal conductance and transverse resistance are expressed in Equations 5 and 6 respectively.

Considering a given number of layers (n), the total longitudinal conductance (S) is defined mathematically as;

$$S = \sum_{i=1}^{n} \frac{h_i}{\rho_i} = \frac{h_1}{\rho_1} + \frac{h_2}{\rho_2} + \cdots \frac{h_n}{\rho_n} \quad 5$$

Considering a given number of layers (n), the total transverse resistance (T) is defined as;

$$TR = \sum_{i=1}^{n} h_i \rho_i = h_1\rho_1 + h_2\rho_2 + \cdots h_n\rho_n \quad 6$$

Considering the longitudinal resistivity (ρ_l), the flow of current is parallel to the layers and is expressed in Equation 7;

$$\rho_l = \frac{\sum_{i=1}^{n} h_i}{\sum_{i=1}^{n} \frac{h_i}{\rho_i}} \quad 7$$

In transverse resistivity, the flow of current is considered to be normal to the layers and given by Equation 8;

$$\rho_t = \frac{\sum_{i=1}^{n} h_i \rho_i}{\sum_{i=1}^{n} h_i} \quad 8$$

In a non-uniform medium, the transverse resistivity is always greater than the longitudinal resistivity and the anisotropy coefficient is greater than one. In a uniform medium, the transverse resistivity is equal to the longitudinal resistivity and the anisotropy coefficient is one (Flathe, 1955; Gernez et al., 2019).

The coefficient of anisotropy (λ) is obtained by the combination of Equations 7 and 8 and given by Equation 9;

$$\lambda = \sqrt{\frac{\rho_t}{\rho_l}} \quad 9$$

According to studies carried out by Zohdy et al. (1974), Shailaja et al. (2016), Ekanem (2020) and Asfahani and Al-Fares (2022), have revealed that the coefficient of anisotropy is always 1.0 for isotropic medium and rarely exceeds 2.0 in most of the geological locations.

- **Porosity, formation factor and tortuosity**

Porosity (ϕ) measures the capability of a geologic formation (rocks/ sediments) to hold water. The porosity of sediments/sedimentary rocks is controlled by the grain sizes and shapes, degree of sorting and cementation. The total porosity of the water-saturated hydrogeologic unit was estimated using Equation 10 according to Ekanem et al. (2019)..

$$\phi = 139.12 * \rho_a - 0.728 \quad 10$$

Where ρ_a is the aquifer resistivity obtained from the surface resistivity data.

The formation factor is a transport property that describes the effect of pore formation on the resistance of the geologic materials and it is expressed as the ratio of bulk resistivity to that of water resistivity as given in Equation 11.

$$F = \frac{\rho_a}{\rho_w} \quad 11$$

Where ρ_a is the aquifer resistivity and ρ_w is the water resistivity estimated using Equation 12.

$$\frac{\rho_a}{\rho_w} = \frac{a}{\phi^m} \rightarrow \rho_w = \frac{\rho_a \phi^m}{a} \quad 12$$

where a and m are Archie constants, a is the pore geometric factor (a = 0.52) and m is the cementation factor (m = 1.54) as estimated in the study by Omeje et al. (2021) according to Archie's equation. The conductivity of water-saturated rock/soil is very sensitive to changes in either of a or m.

Tortuosity (τ) characterises the complex pathways of fluid diffusion and electrical conduction through porous formation, it describes the transport properties of porous formation. It is related to porosity and formation factor in Equation 13.

$$\tau = \sqrt{F\phi} \quad 13$$

- **Hydraulic conductivity (K) and permeability (*Kp*)**

Hydraulic conductivity is a parameter that measures the resistance to the movement of groundwater through a porous formation. The presence of water in the pores of a saturated layer satisfies adhesion and cohesion properties, allowing the free flow of water. Hence, hydraulic conductivity in the saturated layer is greater than that in the unsaturated layer. The hydraulic conductivity is related to porosity as determined from the Kozeny-Carman-Bear's equation given in Equation 14.

$$K = \left(\frac{\delta_w . g}{\mu_d}\right) . \left(\frac{{d_m}^2}{180}\right) . \left(\frac{\phi^3}{(1-\phi)^2}\right) \quad 14$$

Where ϕ is the effective porosity, and g is the acceleration due to gravity ($10 m/s^2$), δ_w is the density of water ($1000 kg/m^3$), d_m is site mean diameter (0.00036m) measured using the micrometre screw gauge, μ_d is the coefficient of dynamic viscosity of water which is approximately 0.0014 kg/ms (Fetters, 1994).

Permeability (K_p) in millidarcy (mD) describes how those pores are shaped and interconnected and measures the capacity of a porous formation to transmit groundwater through a saturated zone. The water transmitting properties (hydraulic conductivity and permeability) relates with effective porosity as in Equation 15.

$$K_p = \frac{\mu_d . K}{\delta_w . g} \quad 15$$

where δ_w is the water density (1000 kgm^{-3}), μ_d is the coefficient of dynamic friction and g is the acceleration due to gravity ($g = 10 m/s^2$).

Description of the study area and its geology

The study area encompasses parts of Nsukka region in southeastern Nigeria, situated within the geographical coordinates ranging from latitudes N to N, and longitudes E to E (see Figure 1) and covers parts of Nsukka, Enugu Ezike, Obukpa, and Eha Alumona. Characterized by undulating topography with elevations exceeding 250 above sea level with a sparse network of surface drainages. Geomorphollogically, the area exhibit prominent landform types: high relief zones and lowland areas. These distinct landforms arise from the interplay of weathering processes and differential erosion acting upon clastic materials, remnant of Nsukka Formation, which constitute the surface layers (Ofomata, 1967; Nnajieze and Eyankware, 2014).

The study area falls within the Anambra sedimentary basin, predominantly composed of rocks dating to the Upper Cretaceous period. The principal geologic formations include the Nsukka Formation and the Ajali Sandstone, with the latter underlying the former (refer to Figure 1). The Nsukka Formation represents a phase of fluvio-deltaic sedimentation initiated during the Maastrichtian and persisting into the Paleocene. It consists of coarse to medium-grained sandstone transitioning upwards into well-bedded blue clay, fine-grained sandstone and carbonaceous shale with thin bands of limestone (Reyment, 1965 and Obi et al, 2001). These geological features influence the hydrogeology, with sandstones providing significant groundwater reservoirs. Conversely, the Ajali Sandstone predominantly consists of medium to coarse-grained sands, often exhibiting white-colouration. According to Agagu et al. (1985), the permeable sandstone readily recharged in its outcrop belt around the Idah-Nsukka-Enugu escarpment. The Nsukka Formation has a prolific aquifer system, sustaining numerous low to moderately productive wells across the

Nsukka area. Itslateritic capping is vesicular nature which is responsible for its porous and permeable nature. Beneath the lateritic caps lie less pervious clay beds, which facilitate the formation of perched aquifers (Obi et al, 2001; Omeje et al., 2021). However, perched aquifers are absent in areas where the lateritic cap has eroded, exposing and the underlying clay bed.

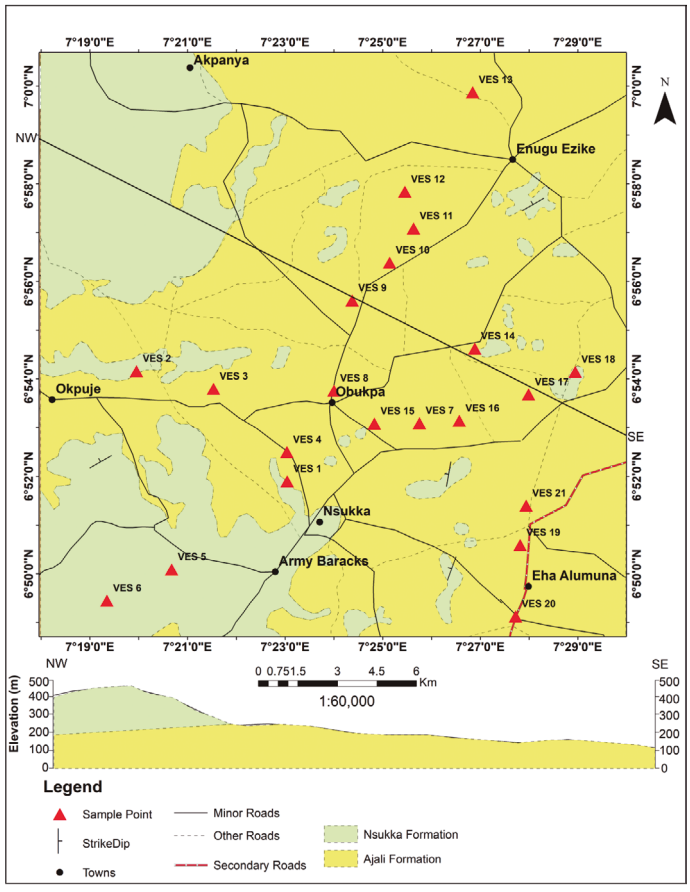

Figure 1. Map describing the geology of the study area

3. Materials and Methods

Twenty-one vertical electrical soundings were acquired for the study using Schlumberger electrode configuration within the maximum current electrode spread, with profiles taken along fairly straight traverses. The IGIS resistivity meter SSR-MP-ATS and its accessories was used for the resistivity survey. The potential difference of the subsurface was measured between the potential electrodes (M and N) while the current was injected into the ground through the current electrodes (A and B). The half current electrodes spread (AB/2) and half potential electrodes spread (MN/2) ranged from 1.0 – 450.0m and 0.25 – 20.0m respectively. Equation 16 was used to calculate the apparent resistivity (ρ_a).

$$\rho_a = G.R_a \qquad 16$$

where G is the geometric factor: $\pi.\left[\frac{\left(\frac{AB}{2}\right)^2-\left(\frac{MN}{2}\right)^2}{MN}\right]$ and R_a is the apparent resistance.

The data were reduced to 1-D geological models using the manual and computer modelling techniques. Plots of ρ_a against AB/2 on a log–log graph were smoothened in order to eliminate noise and associated outliers (Bhattacharya and Patra 1968; Akpan et al., 2006; Chakravarthi et al., 2007). The curve matching technique was employed to interpret the field VES curves (Orellana and Mooney 1966) in order to determine an approximate 1- D models of the resistivities and thicknesses of the corresponding subsurface layers. The WinResist software was used to get correctly the final models of the subsurface layers resistivities, thicknesses, and depths through the set of resistivity curves generated (Zohdy 1989; Zohdy and Bisdorf 1989) as displayed in Figures 2a and b. The various curves display variations in values of resistivity, thicknesses and depths between and within the subsurface layers the current penetrated.

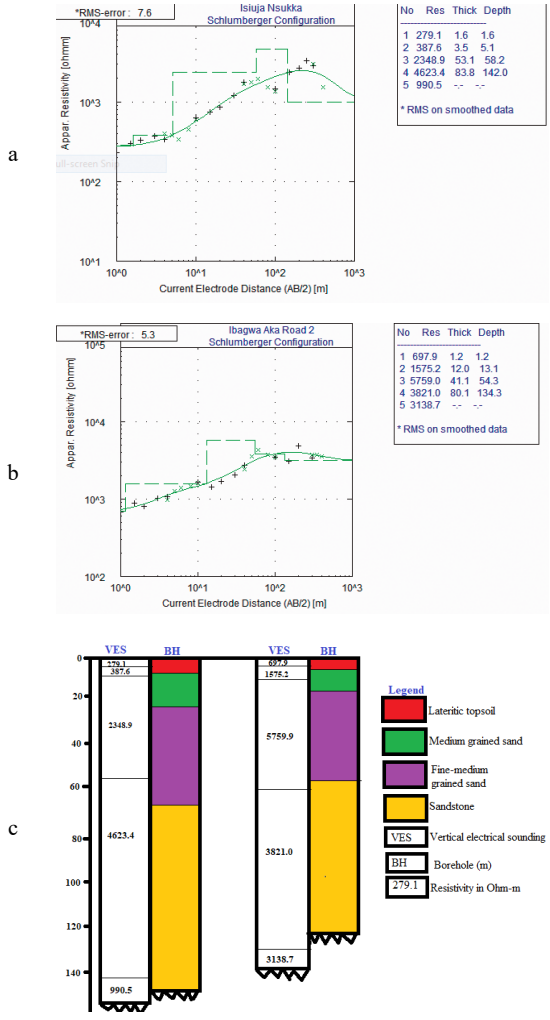

Figure 2. Resistivity curves (a) at VES 11, (b) at VES 21 (c) borehole lithology log

4. Results and Discussion

The inversion results from 21 VES points are presented in Table 1, showing varying values of resistivity, thickness and depth. Five geoelectric layers were delineated across all VES points within the study area's maximum current electrode separation. The delineation of five geoelectric layers suggests a complex subsurface environment with varying lithologies and potential aquifer systems. The interpreted model curves are predominantly of the AKH curve type, comprising about 38% of the total curve types. Other curve types are HKH (4.8%), AAA (14.3%), HAA (9.5%), KQH (14.3%), AAK (9.5%), KHA (4.8%) and AKQ (4.8%), as shown in Table 1. The frequency distribution of the curve types is displayed in Figure 3. The predominance of the AKH curve type suggests the presence of a relatively resistive layer (A) overlying a more conductive layer (K), followed by another resistive layer (H). This configuration might point to a common stratigraphy of dry or less conductive topsoil, followed by a water-bearing layer, and then another resistive layer, possibly indicative of bedrock or compacted sediments. The presence of other curve types, including HKH, AAA, HAA, KQH, AAK, KHA, and AKQ, highlights the variability in the subsurface conditions such as in soil composition, moisture content, rock types, and the presence of fractures or voids. The variability in curve types indicates that the area is geologically diverse, which may affect groundwater flow, and resource management.

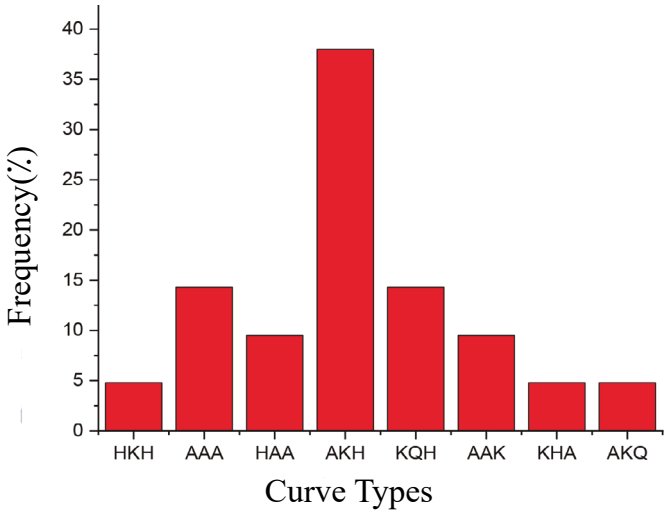

Figure 3. Frequency distribution of curve types

The topmost geo-electric layer has resistivity values ranging from 83.4 to 1277.4 Ωm, with thickness and depth ranging from 0.4 to 2.3 m, respectively. The second and third geoelectric layers are characterised by resistivity values varying from 68.9 to 9395.9 Ωm and 111.3 to 6078.6 Ωm, respectively. The thicknesses of these layers range from 1.5 to 14 .6 m and 2.7 to 54 6 m, respectively, with corresponding depths varying from 2.5 to 15.0 m and 5.2 to 59.1 m. The fourth layer, identified as the saturated units (aquifer units) is characterized by primary geoelectric parameters ranging from 156.8 to 8823.4 Ωm, with thicknesses spanning from 9.6 to 159. 7 m and depths from 28.8 to 180.1 m. This indicates the presence of potentially significant groundwater resources, but with varying quality and quantity. The resistivity of the fifth layer ranges from 990.5 to 13100 Ωm, with thickness and depth undefined. The primary geoelectric parameter from VES were used in empirical relations (equations 5 - 9) to obtain the secondary parameters as shown in Table 2. The wide range of resistivity values within each geoelectric layer suggests a highly heterogeneous subsurface environment, indicating varying lithological compositions and possibly different degrees of weathering or fracturing. The resistivity values were within the range obtained by Ezema et al. (2020), Omeje et al. (2022), Ossai et al. (2023) in their studies.

The resistivity and thickness of the saturated layer vary from 156.8 – 8823.4 Ωm and 9.6 – 112.1 Ωm, respectively, with averages of 2648.16 Ωm and 64.68 m. The distribution of resistivity and thickness of the saturated layer are displayed in the contour maps (Figures 4 and 5). Figure 4 shows the highest resistivity value in the northcentral part of the study area, while in Figure 5 indicates the highest thickness values in the southeastern part of the study area. The spatial variation of these parameters reflects the inhomogeneity of the subsurface geologic materials.

Table 1. Summary of interpreted VES result

VES Sites	Long. (^{O}E)	Latitude (^{O}N)	Layer Resistivity (Ωm)					Thickness (m)				Depth (m)				Elevation (m)	Curve type
			ρ_1	ρ_2	ρ_3	ρ_4	ρ_5	h_1	h_2	h_3	h_4	d_1	d_2	d_3	d_4		
1	7.3843	6.8634	123.4	317.4	1547.6	1021.0	6505.2	1.0	1.5	2.7	71.0	1.0	2.5	5.2	76.2	404	HKH
2	7.3323	6.9005	83.4	500.5	772.0	2451.8	8220.1	0.6	2.7	4.9	95.8	0.6	3.3	8.2	104.0	425	AAA
3	7.3586	6.8948	873.4	2676.8	3464.1	6234.0	7596.6	0.7	5.0	29.5	71.0	0.7	5.7	35.2	106.2	369	AAA
4	7.3863	6.8676	127.0	77.5	111.3	985.3	5672.6	1.0	3.5	54.6	38.9	1.0	4.6	59.1	98.0	449	HAA
5	7.3443	6.8327	389.4	3428.0	6078.6	1361.9	7569.9	1.0	8.7	32.8	72.4	1.0	9.6	42.4	114.7	342	AKH
6	7.3227	6.8231	100.8	496.5	4426.9	786.5	3656.3	0.4	14.6	25.0	53.0	0.4	15.0	40.0	93.0	351	AKH
7	7.4295	6.8843	205.8	996.7	4217.9	2217.7	4115.0	0.8	11.1	11.9	60.3	0.8	11.9	23.8	84.0	338	AKH
8	7.4003	6.8949	972.4	1918.9	4310.0	1384.7	1766.5	2.3	2.8	6.1	112.1	2.3	5.1	11.3	123.4	337	AKH
9	7.4065	6.9247	1277.4	8844.5	1531.1	156.8	2100.7	0.7	3.9	4.4	17.3	0.7	4.6	9.0	26.3	440	KQH
10	7.4193	6.9371	950.0	9395.9	1071.3	204.8	6471.6	0.9	3.4	49.4	57.0	0.9	4.2	53.6	110.6	438	KQH
11	7.4275	6.9493	279.1	387.6	2348.9	4623.4	990.5	1.6	3.5	53.1	83.8	1.6	5.1	58.2	142.0	405	AAK
12	7.4345	6.9603	163.2	871.0	928.6	8823.4	11039.9	1.8	7.9	11.5	80.4	1.8	9.7	21.2	101.6	285	AAK
13	7.4482	6.9964	305.2	877.3	785.2	2184.5	9801.1	1.2	3.8	14.8	9.6	1.2	5.0	19.7	29.3	437	KHA
14	7.4484	7.0093	390.6	2302.2	1733.7	445.6	3221.4	0.4	2.7	4.0	21.7	0.4	3.1	7.1	28.8	452	KQH
15	7.4141	6,8831	306.5	68.9	145.8	1703.8	3486.1	1.8	6.8	9.1	15.3	1.8	8.7	17.7	33.1	315	HAA
16	7.4426	6.8846	84.1	411.1	1005.7	4321.3	11576.0	1.2	5.0	21.7	44.1	1.2	6.1	27.8	71.9	389	AAA
17	7.4668	6.8936	128.7	521.2	3452.1	1567.2	2178.9	0.7	8.6	15.2	57.9	0.7	9.3	24.5	82.4	407	AKH
18	7.4822	6.9008	513.0	760.5	5073.7	3269.2	5408.8	1.7	6.7	14.8	78.2	1.7	8.4	23.3	101.5	386	AKH
19	7.4634	6.8416	160.3	388.0	4296.6	2405.6	8490.5	0.9	6.1	13.3	159.7	0.9	7.1	20.3	180.1	397	AKH
20	7.3459	6.8170	212.9	1254.9	6343.5	5641.9	13100.4	1.0	6.0	26.4	78.5	1.0	7.0	33.4	111.6	355	AKH
21	7.4665	6.9556	697.9	1575.2	5759.0	3821.0	3138.7	1.2	12.0	41.1	80.1	1.2	13.1	54.3	134.3	306	AKQ

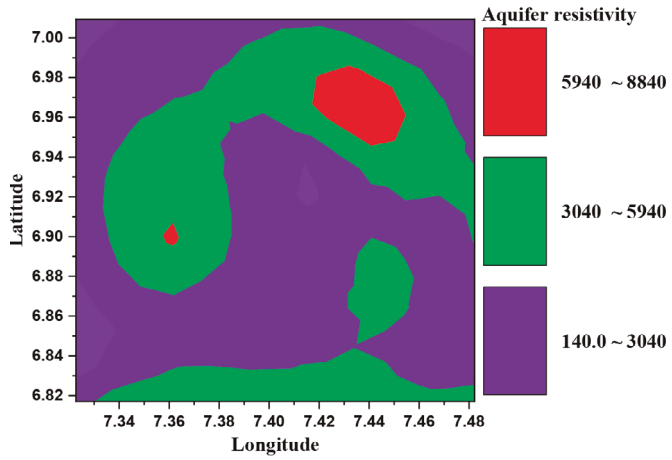

Figure 4. 2D contour map of aquifer resistivity

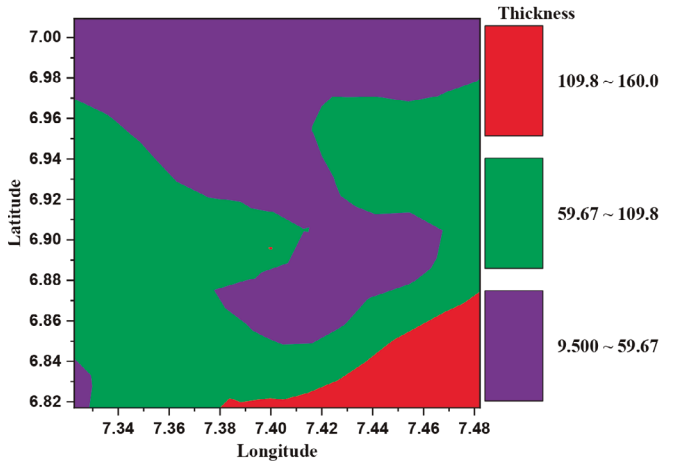

Figure 5. 2D contour map of aquifer thickness

The longitudinal conductance (S) values, varying between 0.01 and 0.54 Ω^{-1} (Figure 6), help determine the protectivity of the study area. According to the classification of Henriet (1976) and Oladapo et al. (2004), the greater part of the study area is poorly protected based on longitudinal conductance values of $<0.1\Omega^{-1}$. Moderate protectivity is observed in the central part of the study area at VES 4, with longitudinal conductance $> 0.5\Omega^{-1}$. Areas with high longitudinal conductance are characterized by relatively thick geologic successions and clayey overburden, which offers protection to the underlying aquifer units from surface contaminants.

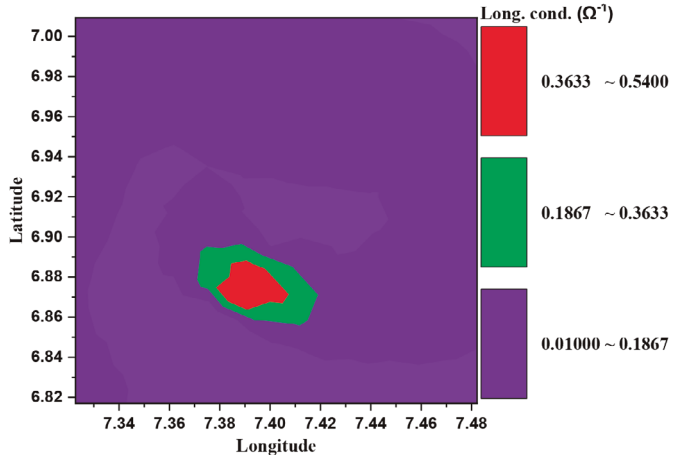

Figure 6. 2D contour map of longitudinal conductance

As posited by Shailaja et al. (2016), and Oguama et al. (2019) the low values of S may be attributed to the absence or minimal amount of clay as an overburden impervious material, allowing easy infiltration of contaminants into the aquifer units. varies between 373.90 and 11375 Ωm^2, with an average value of 4827.56 Ωm^2. The spatial variation of TR (Figure 7) shows that high values in the central, southwestern and southeastern parts of the study area.

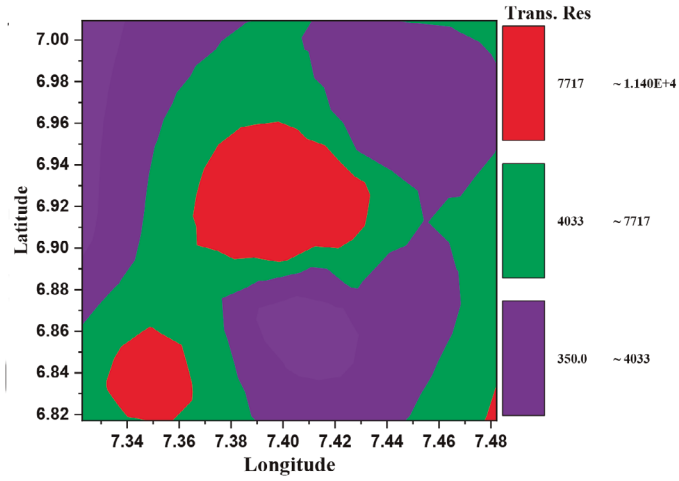

Figure 7. 2D contour map of transverse resistance

The longitudinal resistivity (ρ_l) and transverse resistivity (ρ_t) were computed from equations 7 and 8 respectively. ρ_l has values range from 108.72 - 4046.87 with an average of 1443.04 while ρ_t value range from 109.56 – 5402.14 with an average of 2408.70. The highest and lowest ρ_l and ρ_t are obtained at VES 4 and VES 5. The distributions of both ρ_l and ρ_t (Figures 8 and 9) indicate a direct relationship, where an increase in one leads to a corresponding increase in the other. The combination of ρ_l and ρ_t in equation 9 gives the coefficient of anisotropy (λ), with values ranging from 1.01 to 1.88 and a mean of 1.3. This implies that the subsurface exhibits moderate anisotropy, suggesting variability in the directional properties of the geological materials, which can impact the flow and distribution of groundwater and other subsurface fluids. The distribution of λ is displayed in Figure 10. The ρ_t values are greater than ρ_l at all VES locations, resulting in λ being greater than unity. According to studies by Zohdy et al. (1974), and Bittar and Rodney (1994), the coefficient of anisotropy is generally unity for isotropic medium and rarely exceeds 2.0 in most geological settings. The highest λ values were observed in the southeastern part of the study area, extending towards the southwest. Asfahani and Al-Fares (2022); and Kumar et al. (2014) suggested that, the high anisotropy values indicate the influence of the weathering, alteration processes, and fracturing and suggest better water-holding capacity). Increased hardness and compaction of rocks results in higher anisotropy, correlating with low porosity (Keller and Frischknecht, 1979; Shailaja et al., 2016).

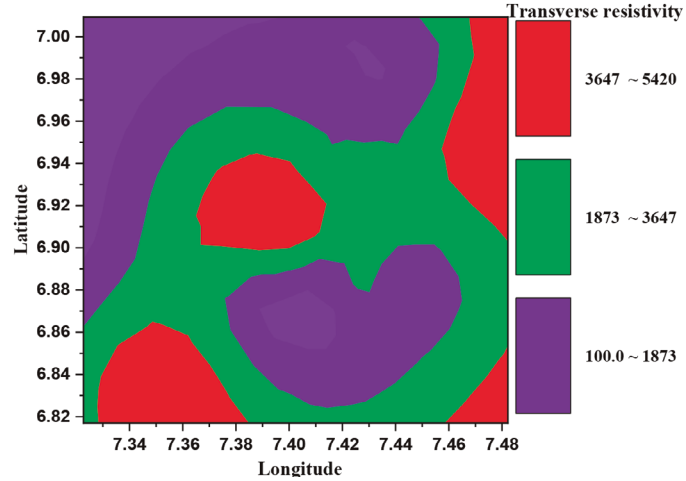

Figure 8. 2D contour map of transverse resistivity

Table 2. Summary of hydrogeological properties

VES Sites	Long. (°E)	Lat. (°N)	ρ_a (Ωm)	h_a (m)	S (Ω^{-1})	TR (Ωm^2)	ρ_t (Ωm)	ρ_l (Ωm)	λ	ϕ	K (m/day)	K_p (mD)	F	τ
1	7.3843	6.8634	1021.0	71.0	0.02	1992.6	918.85	356.79	1.61	0.296	0.897	1.27E-05	3.395	1.002
2	7.3323	6.9005	2451.8	95.8	0.02	1330.14	632.22	433.04	1.21	0.288	0.474	6.72E-06	3.546	1.020
3	7.3586	6.8948	6234.0	71.0	0.01	6786.78	3300.75	3146.99	1.02	0.279	0.240	3.41E-06	3.715	1.018
4	7.3863	6.8676	985.3	38.9	0.54	373.90	109.56	108.72	1.01	0.296	0.921	1.31E-05	3.389	1.002
5	7.3443	6.8327	1361.9	72.4	0.01	9937.50	5402.14	4046.87	1.16	0.293	0.727	1.03E-05	3.444	1.005
6	7.3227	6.8231	786.5	53.0	0.04	5003.32	2949.04	1025.08	1.70	0.298	1.081	1.54E-05	3.351	0.200
7	7.4295	6.8843	2217.7	60.3	0.02	5402.24	2580.72	1333.68	1.39	0.288	0.510	7.23E-06	3.529	1.009
8	7.4003	6.8949	1384.7	112.1	0.01	8474.32	3026.83	2137.50	1.19	0.293	0.719	1.02E-05	3.449	1.005
9	7.4065	6.9247	156.8	17.3	0.01	11278.08	4680.51	2329.98	1.42	0.314	3.509	4.98E-05	3.092	0.986
10	7.4193	6.9371	204.8	57.0	0.05	11375.00	1596.34	1132.40	1.19	0.312	2.889	4.1E-05	3.134	0.988
11	7.4275	6.9493	4623.4	83.8	0.04	3239.66	2174.05	1557.44	1.18	0.282	0.299	4.24E-06	3.660	1.015
12	7.4345	6.9603	8823.4	80.4	0.03	2112.76	842.15	652.64	1.14	0.276	0.187	2.65E-06	3.780	1.021
13	7.4482	6.9964	2184.5	9.6	0.03	2047.34	773.79	730.30	1.03	0.289	0.516	7.31E-06	3.526	1.009
14	7.4484	7.0093	445.6	21.7	0.01	4198.84	1874.22	1576.36	1.09	0.304	1.640	2.33E-05	3.258	0.995
15	7.4141	6.8831	1703.8	15.3	0.17	782.30	132.60	106.00	1.12	0.291	0.618	8.77E-06	3.483	1.007
16	7.4426	6.8846	4321.3	44.1	0.05	1544.42	859.50	581.15	1.22	0.282	0.314	4.45E-06	3.648	1.015
17	7.4668	6.8936	1567.2	57.9	0.03	4087.19	2328.34	930.06	1.58	0.292	0.657	9.32E-06	3.468	1.006
18	7.4822	6.9008	3269.2	78.2	0.02	6727.80	3493.89	1542.47	1.51	0.285	0.385	5.45E-06	3.598	1.012
19	7.4634	6.8416	2405.6	159.7	0.02	4848.27	2938.71	830.89	1.88	0.288	0.481	6.82E-06	3.543	1.010
20	7.3459	6.8170	5641.9	78.5	0.01	7843.70	5245.83	2448.67	1.46	0.280	0.258	3.67E-06	3.697	1.017
21	7.4665	6.9556	3821.0	80.1	0.02	1992.60	4722.56	3296.07	1.20	0.283	0.343	4.87E-06	3.626	1.014

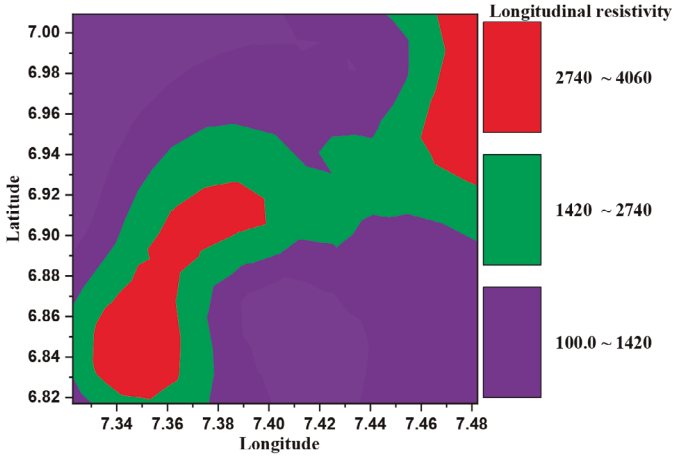

Figure 9. 2D contour map of longitudinal resistivity

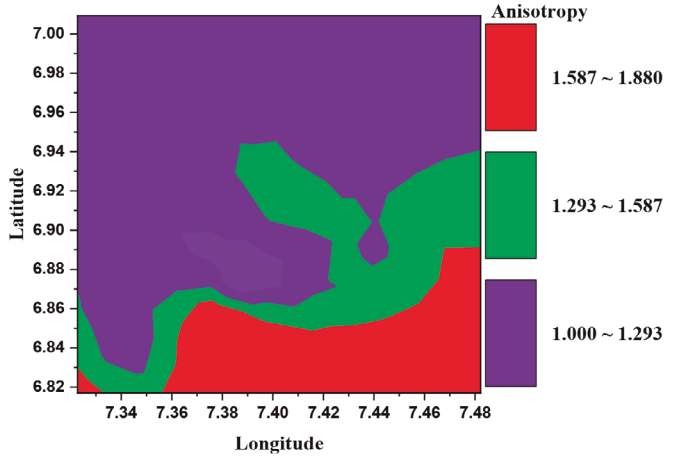

Figure 10. 2D contour map of anisotropy

The estimated fractional porosity (ϕ) reveals that porosity values varies from 0.276 – 0.314, with an average value of 0.291. This indicates a relatively high porosity, suggesting that the material has a significant amount of void space. This could imply good potential for fluid storage and flow. Materials with this porosity range are likely to have good permeability, allowing fluids to move through them relatively easily. Higher porosity is observed in the northeastern parts, extending to the central part of the study area, while low porosity is observed across the southeastern part and extending to the northeastern part. Zones with high porosity correspond to zones with low anisotropy. According to Roscoe (1990), the lithology of the study area is characterized by sand, sandstone and gravel. Figure 11 is a contour map showing the spatial distribution of porosity in the study area. Porosity values relate well with the high and low values of anisotropy, suggesting a positive correlation.

The estimated formation factor (F) ranges from 3.09 – 3.78, with an average of 3.49, The southeastern, western and eastern parts show high formation factor values, decreasing towards the northern part (Figure 12). The results revealed that this parameter trends inversely with porosity, where high porosity leads to a low formation factor and vice-versa. The spatial variation of tortuosity (τ) reveals a range of values from 0.200 – 1.021, with an average of 1.007. The hydraulic conductivity (K) range from 0.187 – 3.780 m/day, while permeability (K_p) values range between 1.02E-05 and 9.32E-06 mD. The spatial distributions of these parameters from the contour maps generated show similar patterns (Figure 13 and 14), with low values are observed in the south, extending to the northeast. Hydraulic conductivity and permeability are controlled by intergranular porosity and fracturing, suggesting that parts with low low K and K_p may be due to poor pore spaces communication channels and grain size variations (Ibanga and George, 2016; George et al. 2018; Ibuot and Obiora, 2021). Locations displaying high hydraulic conductivity and permeability values will have good groundwater potential, while relatively low values indicate poor groundwater potential in the aquifer system (Ibuot et al. 2019; Ekanem et al. 2022).

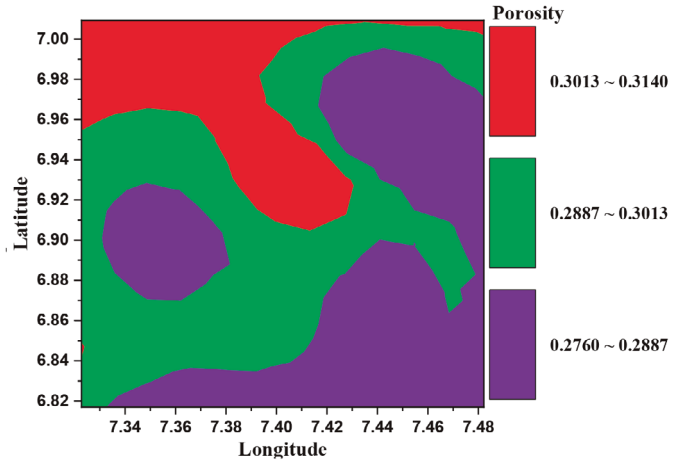

Figure 11. 2D contour map of fractional porosity

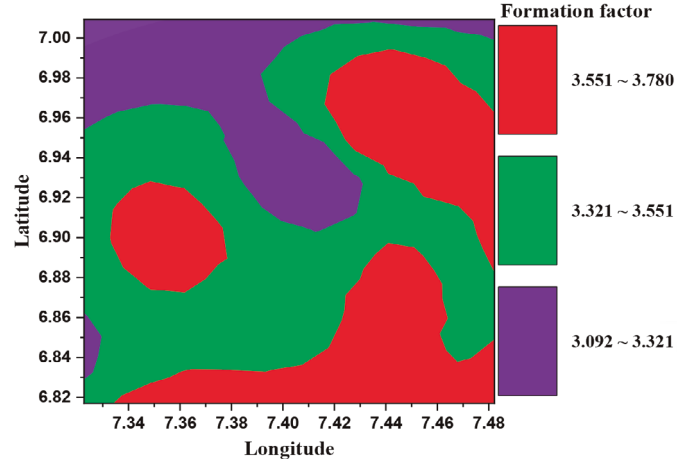

Figure 12. 2D contour map of formation factor

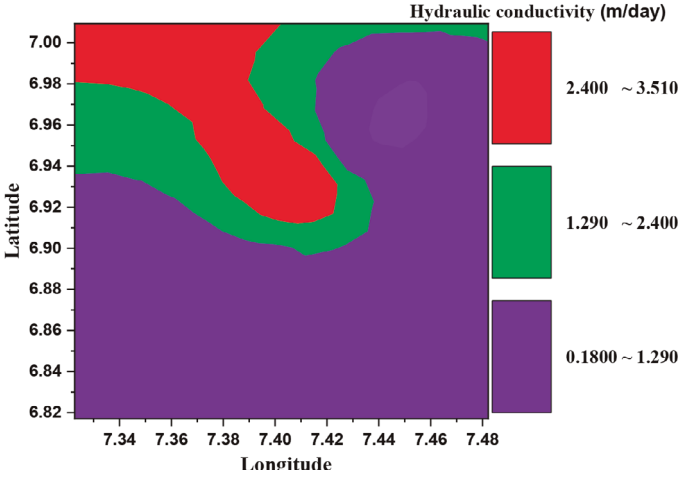

Figure 13. 2D contour map of hydraulic conductivity

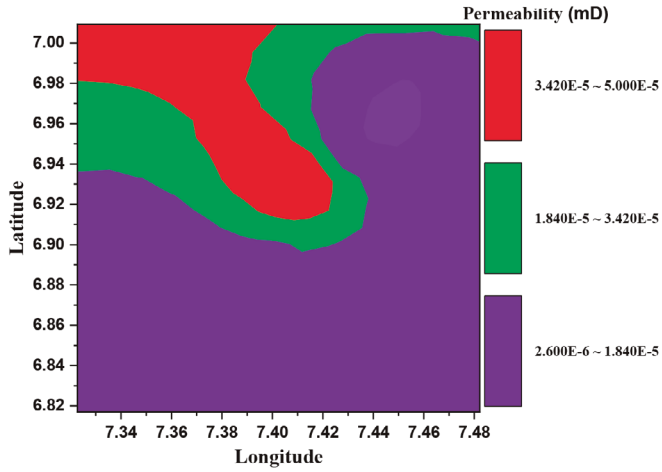

Figure 14. 2D contour map of permeability

Regression Analysis

The results of the estimated parameters were plotted to determine their correlation and relationships. The plot of hydraulic conductivity against porosity (Figure 15a) reveals a power expression with a high correlation coefficient expressed as K = 8.09E11*^22.6 (Equation 17).

From the plot, it is evident that an increase in porosity leads to an increase in hydraulic conductivity, aligning with the variation in the contour maps of Figures 11 and 13. This is expected as hydraulic conductivity depends on pore size, spatial distribution and connectivity.

$$K = 8.09E11*^{22.6} \quad (17)$$

Similarly, Figure 15b shows a power relation between permeability and porosity with a high correlation coefficient, given by given by $Kp = 1.15*\phi^{22.6}$ ((Equation 18).

This indicates that ability is directly related to porosity, suggesting that higher porosity leads to higher permeability, which enhances groundwater transmissibility through interconnected pores.

$$Kp = 1.15*\phi^{22.6} \quad (18)$$

The correlation between the hydraulic conductivity and aquifer resistivity is represented in Figure 15c with a power equation:

$$K = 139.18*\rho a^{-0.73} \quad (19)$$

Additionally, the variability of the aquifer units is expressed through a plot between porosity and aquifer resistivity (Figure 15d), yielding a power equation with strong correlation coefficient:

$$\phi = 0.37*\rho a^{-0.03} \quad (20)$$

Finally, the formation factor-porosity (Figure 15e) provides a power expression, showing an exponential decrease in formation factor with increasing porosity, with a strong correlation coefficient.

$$F = 0.52*\phi^{-1.54} \quad (21)$$

The results from this study provide a comprehensive understanding of the subsurface geoelectric layers, indicating a complex and heterogeneous environment with varying lithologies and potential aquifer systems. These findings can inform future research by guiding the development of more accurate predictive models for groundwater exploration, particularly in geologically similar regions. Moreover, the study's insights into resistivity, anisotropy, and porosity can be applied in practical hydrogeology to enhance groundwater management, optimize drilling locations, and assess contamination risks, ultimately improving resource management and environmental protection.

The delineation of multiple geoelectric layers and the variety of curve types observed in this study indicate a highly heterogeneous subsurface, with varying lithologies and aquifer potentials. Modern geophysical techniques, such as 3D resistivity imaging, time-domain electromagnetic (TEM) surveys, and seismic methods, could provide more detailed and continuous subsurface models. These techniques can overcome the limitations of traditional 1D methods like Vertical Electrical Sounding (VES) by offering better resolution and spatial coverage, leading to more accurate delineation of aquifer boundaries and stratigraphic layers. Additionally, integrating advanced data processing techniques such as machine learning algorithms could enhance the interpretation of complex datasets. These algorithms could identify patterns and correlations within large datasets, such as those obtained from multi-dimensional geophysical surveys, leading to more accurate predictions of groundwater potential, aquifer properties, and the spatial distribution of subsurface features.

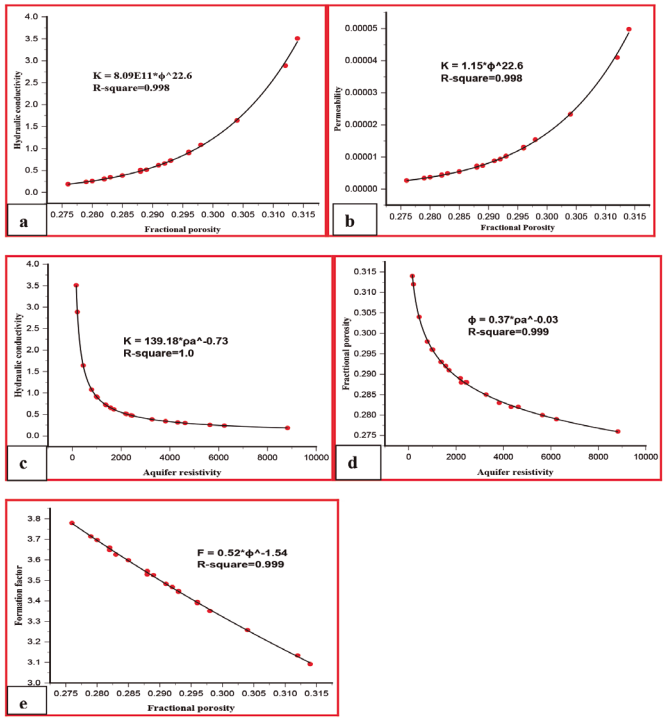

Figure 14(a-e). A graph of (a) hydraulic conductivity against fractional porosity, (b) permeability against fractional porosity, (c) hydraulic conductivity against aquifer resistivity, (d) fractional porosity against aquifer resistivity, (e) formation factor against fractional porosity.

Conclusion

The present study investigated the electro-geohydraulic properties through the qualitative interpretation of resistivity data from twenty-one VES locations across the study area. The analysis identified five geoelectric layers, each with distinct resistivity profiles reflecting the variations in the subsurface lithostratigraphy. Notably, the fourth layer emerged as the main economic aquifer, suggesting it as a prime target for groundwater extraction. The saturated (aquifer) layer, characterized by wide ranges of resistivity, thickness, and depth, indicates substantial variation in aquifer properties.

The study utilized electrical parameters to estimate secondary parameters, which facilitated a detailed interpretation of the subsurface lithological characteristics. The longitudinal conductance indicated that the aquifer's protective capacity ranges from poor to moderate, signifying a minimal presence of clayey or silty layers, thus making it susceptible to contamination. Anisotropy values pointed to a higher water-holding capacity, attributed to processes such as weathering, alteration, and fracturing. The effective porosity analysis revealed that the aquifer comprises primarily unconsolidated materials, such as sandstone and sand-gravel mixtures. The distribution of porosity inversely correlates with anisotropy, highlighting zones of high porosity and low anisotropy, which align with the sandy and gravelly lithology of the area. The variation in hydraulic conductivity and permeability, controlled by intergranular porosity and fracturing, points to areas with good and poor groundwater potential. Higher hydraulic conductivity and permeability values are associated with better groundwater prospects.

The parameter maps illustrated the spatial distribution and variations across the study area, aiding in the delineation of regions with differing aquifer properties. Additionally, these maps highlighted the inverse and direct relationships among various parameters. Regression analysis demonstrated linear and nonlinear correlations among the parameters, all exhibiting positive correlation coefficients. This study underscores the utility of the 1-D resistivity technique in providing valuable insights into subsurface lithostratigraphy. The findings contribute significantly to groundwater exploration and management, demonstrating the technique's potential for effective subsurface characterization.

Acknowledgement

The authors are grateful to members of the Atmospheric and Solid Earth Geophysics Research Group, University of Nigeria, Nsukka for their support and encouragement. The authors also acknowledge the anonymous reviewer(s) and the editor(s) for their insightful comments and suggestions which have helped to improve the quality of this manuscript.

Reference

Agagu, O. K., Fayose, E. A., & Petters, S. W. (1985). Stratigraphy and sedimentation in the Senonian Anambra Basin of eastern Nigeria. *Journal Mining and Geology*, 22(1), 26 –36.

Akpan, F. S., Etim O. N., & Akpan, A. E. (2006). Geoelectrical investigation of groundwater potential in parts of Etim Ekpo local government area, Akwa Ibom State. *Nigerian Journal of Physics,* 18, 39 - 44.

Akpan, A. E., Ugbaja, A. N., & George, N. J. (2013). Integrated geophysical, geochemical and hydrogeological investigation of shallow groundwater resources in parts of the Ikom-Mamfe Embayment and the adjoining areas in Cross River State, Nigeria. *Environmental Earth Science,* 70(3), 1435 - 1456.

Asfahani, J., & Al-Fares, W. (2021). Alternative vertical electrical sounding technique for hydraulic parameters estimation of the quaternary basaltic aquifer in Deir Al-Adas area, Yarmouk Basin, Southern Syria. *Acta Geophysica,* 69, 1901–1918.

Batayneh, A. T. (2009). A hydrogeophysical model of the relationship between geoelectric and hydraulic parameters, Central Jordan. *Journal of water Resources Protection,* 1400 – 407

Bhattacharya, P. K., & Patra, H. P. (1968). *Direct Current geoelectric sounding.* Elsevier, Amsterdam.

Bittar, M. S., & Rodney, P. F. (1994). *The effects of rock anisotropy on MWD electromagnetic wave resistivity sensors.* Proceedings SPWLA 35th Ann. Logg. Symp. Tulsa, USA.

Bricker, S. H., Banks, V. J., Galik, G., Tapete, D., & Jones, R. (2017). Accounting for groundwater in future city visions. *Land Use Policy*. https://doi.org/10.1016/j.landusepol.2017.09.018

Chakravarthi, V., Shankar, G. B. K., Muralidharan, D., Harinarayana, T., & Sundararajan, N. (2007). An integrated geophysical approach for imaging

sub-basalt sedimentary basins: case study of Jam River basin, India. *Geophysics*, 72(6), B141–B147.

Ekanem, A. E., George, N. J., Thomas, J. E., & Nathaniel, E. U. (2019). Empirical Relations Between Aquifer Geohydraulic–Geoelectric Properties Derived from Surficial Resistivity Measurements in Parts of Akwa Ibom State, Southern Nigeria. *Natural Resources Research*, 29, 2635–2646. https://doi.org/10.1007/s11053-019-09606-1

Ekanem, A. M. (2020). Georesistivity modelling and appraisal of soil water retention capacity in Akwa Ibom State University main campus and its environs, Southern Nigeria. *Modelling Earth System and Environment,* 6, 2597-2608. https://doi.org/10.1007/s40808-020-00850-6

Ekanem, K. R., George, N. J. & Ekanem, A. M. (2022). Parametric characterization, protectivity and potentiality of shallow hydrogeological units of a medium-sized housing estate, Shelter Afrique, Akwa Ibom State, Southern Nigeria. *Acta Geophysica*. https://doi.org/10.1007/s11600-022-00737-3

Ekwe, A. C., Opara, A. I., Okeugo, C. G., Azuoko, G., Nkitman, E. E., Abraham, E. M., Chukwu, C. G., & Mbaeyi, G. (2020). Determination of aquifer parameters from geo-sounding data in parts of Afikpo Sub-basin Southeastern Nigeria. *Arabian Journal of Geosciences*, 13, 189. https://doi.org/10.1007/s12517-020-5137-y

Ezema,O. K., Ibuot, J. C., & Obiora, D. N. (2020), Geophysical investigation of aquifer repositories in Ibagwa Aka, Enugu State, Nigeria, using electrical resistivity method. *Groundwater for Sustainable Development,* 11(100458).

Fetters, C. W. (1994). *Applied Hydrogeology.* 3rd edn. Prentice Hall Inc, New Jersey, pp. 600.

Flathe, H. (1955). Possibilities and limitations in applying geoelectrical methods to hydrogeological problems in the coastal area of northwest Germany. *Geophysical Prospecting,* 3(95), 110.

George, N. J. (2020). Appraisal of hydraulic flow units and factors of the dynamics and contamination of hydrogeological units in the littoral zones: a case study of Akwa Ibom State University and its Environs, Mkpat Enin LGA, Nigeria. *Natural Resources Research, 29, 3771–3788.* https://doi.org/10.1007/s11053-020-09673-9

George, N. J., Ibuot, J. C., & Obiora, D. N. (2015). Geoelectrohydraulic parameters of shallow sandy aquifer in Itu, Akwa Ibom State (Nigeria) using geoelectric and hydrogeological measurements. *Journal of African Earth Sciences,* 110, 52–63.

George, N. J., Ibuot, J. C., Ekanem, A. M., & George, A. M. (2018). Estimating the indices of inter- transmissibility magnitude of active surficial hydrogeologic units in Itu, Akwa Ibom State, Southern Nigeria. *Arabian Journal of Geosciences,* 11(6), 1–16.

Gernez, S, Bouchedda, A., Gloaguen, E., & Paradis, D. (2019). Comparison between hydraulic conductivity anisotropy and electrical resistivity anisotropy from tomography inverse modelling. *Frontiers in Environmental Science,* 7, 67.

González-Álvarez, I., Ley-Cooper, A., & Salama, W. (2016). A geological assessment of airborne electromagnetics for mineral exploration through deeply weathered profiles in the southeast Yilgarn Cratonic margin, Western Australia. Ore Geology Reviews, 73, 522-539. https://doi.org/10.1016/j.oregeorev.2015.10.029

Henriet, J. P. (1976). Direct application of Dar-Zarrouk parameters in ground water surveys. *Geophysical Prospecting,* 24, 344–353.

Ibanga, J. I., & George, N. J. (2016). Estimating geohydraulic parameters, protective strength, and corrosivity of hydrogeological units: a case study of ALSCON, Ikot Abasi, Southern Nigeria. *Arabian Journal Geoscience*, 9, 363.

Ibuot, J. C., & Obiora, D. N. (2021). Estimating geohydrodynamic parameters and their implications on aquifer repositories: a case study of University of Nigeria, Nsukka, Enugu State. *Water Practice and Technology,* I6(1),162 – 181.

Ibuot, J. C., Aka, M. U., Inyang, N. J., & Agbasi, O. E. (2022). Georesistivity and physicochemical evaluation of hydrogeologic units in parts of Akwa Ibom State, Nigeria. *International Journal of Energy and Water Resources*. https://doi.org/10.1007/s42108-022-00191-3

Ibuot, J. C., George, N. J., Okwesili, A. N., & Obiora, D. N. (2019). Investigation of litho-textural characteristics of aquifer in Nkanu West Local Government Area of Enugu state, southeastern Nigeria. *Journal of African Earth Science,* 153, 197–207.

Ibuot, J. C., Obiora, D. N., & George, N. J. (2024). Estimating geohydraulic response parameters from electrical resistivity data in tertiary-quaternary hydro-lithofacies in Uyo, Southern Nigeria. *Applied Water Sciences*, 14, 9 https://doi.org/10.1007/s13201-023-02057-3

Kelbe, B. E., Taylor, R. H., & Haldorsen, S. (2011). Groundwater hydrology. In: Perissinotto, R., Stretch, D., & Taylor, R. H. (Eds.) *Ecology and Conservation of Estuarine Ecosystems: Lake St Lucia as a Global Model*, 151-168. https://doi.org/10.1017/CBO9781139095723.010

Keller, G. V. & Frischknecht, F. C. (1966). *Electrical methods in geoelectric prospecting*. Pergamon Press, 90–04.

Lowrie, W. (1997). *Fundamentals of Geophysics*. Cambridge University Press, New York, NY.

Mazac, O., Kelly, W. E., & Landa, I. (1985). A Hydrogeophysical model for relation between electrical and hydraulic properties of aquifers. *Journal of Hydrology,* 79, 1–19.

Metwaly, M., El-Alfy, M., Eawaad, E., Ismail, A., & El-Qady, G. (2014). Estimating aquifer hydraulic parameters from electrical resistivity measurements: a case study at Khuf Formation Aquifer, Al Quwy'yia Area, Central of Saudi Arabia. *International Conference on Engineering Geophysics, Al Ain, United Arab Emirates*. https://doi.org/10.1190/iceg2015-060

Niwas, S., & Celik, M. (2012). Equation estimation of porosity and hydraulic conductivity of Ruhrtal aquifer in Germany using near surface geophysics. *Journal Applied Geophysics,* 84, 77–85.

Niwas, S., & Singhal, D. C. (1981). Estimation of aquifer transmissivity from Dar-Zarrouk parameters in porous media. *Journal of Hydrology,* 50, 393–399.

Nnajieze, V. S., & Eyankware, M. O. (2014). Lithofacies and paleodepositional environment of okpuje and its environs nsukka north east local government of Enugu state, south eastern Nigeria. *International Journal of Innovation and Scientific Research,* 12(2), 453-462.

Nugraha, G. U., Bakti, H., Lubis, R. F., Sudrajat, Y., & Arisbaya, I. (2021). Aquifer vulnerability in the Coastal Northern Part of Lombok Island Indonesia. *Environment, Development and Sustainability,* 24, 1390-1410. https://doi.org/10.1007/s10668-021-01459-0.

Obi,G. C., Okogbue, C. O., & Nwajide, C. S. (2001). Evolution of the Enugu Cuesta: A tectonically driven erosional process. *Global Journal of Pure and Applied Sciences,* 7(2), 321–330.

Obiora, D. N., Ajala, A. E., & Ibuot, J. C. (2015) Evaluation of aquifer protective capacity of overburden unit and soil corrosivity in Makurdi, Benue state, Nigeria, using electrical resistivity method. *Journal of Earth System Science,* 124(1), 125–135.

Obiora, D. N., Ibuot, J. C., & George, N. J. (2016). Evaluation of aquifer potential, geoelectric and hydraulic parameters in Ezza North, Southeastern Nigeria, using geoelectric sounding. *International Journal of Environmental Science and Technology,* 13(2), 435–444.

Obiora, D. N., & Ibuot, J. C. (2020). Geophysical assessment of aquifer vulnerability and management: A case study of University of Nigeria, Nsukka. Enugu State. *Applied Water Science,* 10(1), 1–11.

Obiora, D. N., & Ibuot, J. C. (2023). Electrical geophysical evaluation of susceptibility to flooding in University of Nigeria, Nsukka main campus and its environs, Southeastern Nigeria. *Journal of Groundwater Science and Engineering,* 11(2023), 422–434.

Omeje, E. T., Ibuot, J. C., Ugbor, D. O., & Obiora, D. N. (2022). Geophysical investigation of transmissibility and hydrogeological properties of aqui-

fer system: a case study of Edem, Eastern Nigeria. *Water Supply,* 22(5), 5044 – 5055.

Ossai, M. N., Okeke, F. N., Obiora, D. N., & Ibuot, J. C. (2023). Evaluation of groundwater repositories in parts of Enugu, Eastern Nigeria via electrical resistivity technique. *Applied Water Science,* 13, 64. https://doi.org/10.1007/s13201-022-01839-5

Ofomata, G. E. K. (1967). Some Observations on Relief and Erosion in Eastern Nigeria. *Revue de Geomorph, Dynamise*, XVU, 21-29.

Oguama, B. E., Ibuot, J. C., Obiora, D. N., & Aka, M. U. (2019). Geophysical investigation of groundwater potential, aquifer parameters, and vulnerability: a case study of Enugu State College of Education (Technical). *Modelling Earth System Environment,* 5, 1123–1133.

Oladapo, M. I., Mohammed, M. Z., Adeoye, O. O., & Adetola, B. A. (2004). Geo-electrical investigation of the Ondo state housing corporation estate Ijapo Akure, Southwestern Nigeria. *Journal of Mining and Geology,* 40(1), 41–48.

Oli, I. C., Ahairakwem, C. A., Opara, A. I., Ekwe, A. C., Osi-Okeke, I., Urom, O. O., et al. (2020). Hydrogeophysical assessment and protective capacity of groundwater resources in parts of Ezza and Ikwo areas, southeastern Nigeria. *International Journal of Energy and Water Resources,* 5, 57-72. https://doi.org/10.1007/s42108-020-00084-3

Omeje, E. T., Ibuot, J. C., Ugbor, D. O., & Obiora, D. N. (2022a). Geophysical investigation of transmissibility and hydrogeological properties of aquifer system: a case study of Edem, Eastern Nigeria. *Water Supply,* 22(5), 5044–5055.

Omeje, E. T., Obiora, D. N., Okeke, F. N., Ugbor, D. O., Ibuot, J. C., & Akpan, A. S. (2022b). Aquifer flow unit analysis using stratigraphic modified Lorenz plot: a case study of Edem, eastern Nigeria. *Journal of Engineering and Applied Science,* 69, 33. https://doi.org/10.1186/s44147-022-00081-9

Omeje, E. T., Ugbor, D. O., Ibuot, J. C., & Obiora, D. N. (2021). Assessment groundwater repositories in Edem, Southern Nigeria, using vertical electrical sounding. *Arabian Journal of Geosciences,* 14, 421.

Opara, A. I., Eke, D. R., Onu, N. N., Ekwe, A. C., Akaolisa, A. C., Okoli, A. E. & Inyang, G. E. (2020). Geo-hydraulic evaluation of aquifers of the Upper Imo River Basin, Southeastern Nigeria using Dar-Zarrouk parameters. *International Journal of Energy and Water Resources*,5, 259-275. https://doi.org/10.1007/s42108-020-00099-w

Orellana, E., & Mooney, H. M. (1966). *Master Tables and curves for vertical electrical sounding over layered structures*. Interciencia, Madrid.

Reyment, R. A. (1965). *Aspect of the Geology of Nigeria*. Ibadan Univ. Press. pp 133.

Roscoe, M. C. (1990). *Handbook of Ground Water Development*. John Wiley and Sons, New-York. ISBN 10: 0471856118/ ISBN 13: 9780471856115.

Shailaja, G., Laxminarayana, M., Patil, J. D., Erram, V. C., Suryawanshi, R. A., & Gupta, G. (2016). Efficacy of anisotropic properties in groundwater exploration from geoelectric sounding over trap covered terrain. *Journal of Indian Geophysical Union*, 20(5), 453–461.

Shishaye, H. A., Tait, D. R., Befus, K. M., & Maher, D. T. (2019). An integrated approach for aquifer characterization and groundwater productivity evaluation in the Lake Haramaya watershed, Ethiopia. *Hydrogeology Journal,* 27, 2121-2136. https://doi.org/10.1007/s10040-019-01956-7

Telford, W. M., Geldart, L. P., Sheriff, R. E., & Keys, D. A. (1990) *Applied Geophysics.* Cambridge University Press, Cambridge.

Todd, D. K., & Mays, L. W. (2005). *Groundwater hydrology*. Hoboken, NJ: Wiley.

Umar, N. D., & Igwe, O. (2019). Geoelectric method applied to groundwater protection of a granular sandstone aquifer. *Applied Water Science,* 9, 112.

Zohdy, A. A. R. (1989). A new method for the automatic interpretation of Schlumerger and Wenner sounding curves. *Geophysics*, 54, 245–253.

Zohdy, A. A. R., & Bisdorf, R. J. (1989). *Programs for the automatic processing and interpretation of Schlumberger sounding curves in Quick Basic*. US Geol Surv Open File Rep 89(13), 64.